HHS Public Access

Author manuscript

Brain Stimul. Author manuscript; available in PMC 2019 May 01.

Published in final edited form as:

Brain Stimul. 2018 ; 11(3): 607–617. doi:10.1016/j.brs.2018.01.028.

Pallidal deep brain stimulation modulates excessive cortical high β phase amplitude coupling in Parkinson disease

Mahsa Malekmohammadi[a], **Nicholas AuYong**[a], **Joni Ricks-Oddie**[b], **Yvette Bordelon**[c], and **Nader Pouratian**[a,d,e,f]

[a]Department of Neurosurgery, University of California, Los Angeles, CA, USA

[b]Institute for Digital Research and Education (IDRE), University of California, Los Angeles, CA, USA

[c]Department of Neurology, University of California, Los Angeles, CA, USA

[d]Department of Bioengineering, University of California, Los Angeles, CA, USA

[e]Neuroscience Interdepartmental Program, University of California, Los Angeles, CA, USA

[f]Brain Research Institute, University of California, Los Angeles, CA, USA

Abstract

Objective—Deep brain stimulation (DBS) of the subthalamic nucleus (STN) and globus pallidus internus (GPi) are equally efficacious in the management of Parkinson disease (PD). Studies of STN-DBS have revealed a therapeutic reduction in excessive cortical β-γ phase-amplitude coupling (PAC). It is unclear whether this is specific to STN-DBS and potentially mediated by modulation of the hyperdirect pathway or if it is a generalizable mechanism seen with DBS of other targets. Moreover, it remains unclear how cortical signals are differentially modulated by movement versus therapy. To clarify, the effects of GPi-DBS and movement on cortical β power and β-γ PAC were examined.

Methods—Right sensorimotor electrocorticographic signals were recorded in 10 PD patients undergoing GPi-DBS implantation surgery. We evaluated cortical β power and β-γ PAC during blocks of rest and contralateral hand movement (finger tapping) with GPi-DBS off and on.

Results—Movement suppressed cortical low β power (P=0.008) and high β-γ PAC (P=0.028). Linear mixed effect modeling (LMEM) showed that power in low and high β bands are differentially modulated by movement (P=0.022). GPi-DBS also results in a significant suppression of high β-γ PAC but without power modulation in either β sub-band (P=0.008). Cortical high β-γ PAC is significantly correlated with severity of bradykinesia (Rho=0.59, P=0.045) and changes proportionally with therapeutic improvement (Rho=0.61, P=0.04).

Corresponding Author: Mahsa Malekmohammadi, PhD, UCLA Neurosurgery, 300 Stein Plaza Suite 464, Los Ángeles, CA 90095, 310-206-2189, FAX 310-794-1848, mmalekmohammadi@mednet.ucla.edu.

Conclusions—Similar to STN-DBS, GPi-DBS reduces motor cortical β-γ PAC, like that also reported with dopaminergic mediations, suggesting it is a generalizable symptom biomarker in PD, independent of therapeutic target or proximity to the hyperdirect pathway.

Keywords

Parkinson disease; Deep brain stimulation; Globus Pallidus internus; Motor cortex; Phase amplitude coupling

Introduction

In Parkinson disease (PD), excessive β oscillations (13–35 Hz) have been described at multiple nodes throughout basal ganglia-thalamocortical (BGTC) motor network [1–8]. A fundamental issue to understanding PD pathophysiology is to clarify how neuronal oscillations relate to the symptoms and change in response to the therapy such as dopaminergic medications or deep brain stimulation (DBS). One proposed concept is that motor symptoms in PD emerge from abnormal information transmission across the BGTC circuit [9–11]. DBS has been shown to regularize information transmission in movement disorders by reducing the entropy in the neuronal firing patterns [9,10,12,13]. This phenomenon may be reflected in the higher order interactions seen in phase-amplitude coupling (PAC), where the phase of a low-frequency oscillation is coupled to the amplitude of higher frequency oscillations.

In PD, motor cortical β-γ PAC is exaggerated compared to patients with dystonia [14] and epilepsy [15] or healthy controls [16]. Furthermore, subthalamic nucleus (STN) DBS suppresses excessive cortical β-γ PAC without modulating cortical β power [17]. While raising the prospect of its use as a disease biomarker, studies have also indicated that motor cortical β-γ PAC is modulated by movement [15,17], potentially limiting its utility as a biomarker.

In addition to recent insights into cortical PAC in PD, there is converging evidence suggesting functional separation of the β band into discrete “low” (13–20 Hz) and “high” (20–35 Hz) sub-bands [18]. Treatment (dopaminergic or STN-DBS) preferentially modulates low β signals in the STN [8,19]. Moreover, PAC within STN is confined to the low β range (low β-HFO) [18]. Likewise, we have recently shown similar subcortical PAC exists in the GPi with a preferred phase encoding rhythm in the low β range [20]. Finally, the preferred frequency of the coupling for motor cortical β-γ PAC differs between PD (high β) and essential tremor (α, 8–12 Hz)/low β) [15]. Such sub-β band functionalities likely suggest different roles for low vs high β in BGTC sub-circuits.

While STN- and GPi-DBS outcomes differ with respect to medication requirement and neurocognitive side effects, both targets are equally efficacious in management of the cardinal motor symptoms of PD [21–23]. But, most studies on DBS mechanisms have been conducted with STN-DBS. While the STN has hyperdirect cortical projections [24], there are no known monosynaptic connections between GPi and cortex. Studying the effect of GPi-DBS on cortical physiology provides a unique opportunity to understand target-specific

versus generalizable mechanisms of DBS, particularly at the network level. This will complement findings that dopaminergic medications likewise modulate cortical PAC [16].

We hypothesized that GPi-DBS, like previously reported for STN-DBS and dopaminergic medications, suppresses motor cortical β-γ PAC, suggesting this effect is not directly mediated by the hyperdirect pathway, rather it is a network-level effect of therapeutic stimulation. We also hypothesized a significant movement-modulation of these signals, but that movement and GPi DBS would differentially affect distinct β sub-bands. To test our hypotheses, we evaluated electrocorticography (ECoG) recordings from sensorimotor cortices during GPi-DBS implantation surgery.

Methods

Patients and surgical procedure

Ten right-handed subjects with idiopathic PD undergoing bilateral GPi-DBS lead implantation provided written informed consent, as approved by the UCLA institutional review board. Table 1 summarizes the demographic and stimulation parameters. All medications were withdrawn at least 12 hours prior to the surgical procedure. DBS leads were targeted to the motor GPi (ventral posterolateral GPi, 2–4 mm anterior, 19–24 mm lateral and 4–6 mm inferior to the mid-commissural point) with intraoperative microelectrode recording and intraoperative awake macro-stimulation confirmation.

All subjects underwent clinical pre-and post-operative imaging. Pre-operative imaging included 3T, T1-weighted magnetization prepared rapid acquisition gradient echo (MPRAGE) image (slice thickness=1 mm, TR=2100 ms, TE=2.98 ms, flip angle=15°). A Laksell stereotactic head frame (Elekta Instruments) was applied and a full head computed tomography scan was obtained (1-mm slice thickness, Siemens Sensation 64). Prior to right-sided DBS lead implantation, an 8-contact ECoG strip (platinum-iridium 4 mm contacts with 1 cm spacing, AdTech Medical) was introduced subdurally via the right frontal burr hole. After DBS lead implantation, a lateral fluoroscopy image was acquired to confirm electrode placement. The subdural strip was removed prior to final anchoring of the DBS lead. Post-operative CT scan was further used to verify final lead position. Anatomical localization of the ECoG strip was performed according to the previously described method [25,26]. Pre and post-operative CT scans were co-registered to pre-operative structural MRI using normalized mutual information and resliced in the Statistical Parameter Mapping (SPM 12) toolbox (visually inspected for accuracy). The cortical surface was reconstructed from the MRI using Freesurfer [27]. A 3D surface of skull and stereotactic frame was rendered from co-registered pre-operative CT scan in the Osirix software [28]. DBS electrodes were reconstructed from the post-operative CT scan and stereotactic frame landmarks were identified on the co-registered pre-operative CT scan. The 2D fluoroscopic image and 3D skull surface were visually inspected and fused using a custom made Matlab GUI and camera toolbox [25]. Reconstructed DBS leads, and stereotactic frame landmarks were used to ensure maximal accuracy of 3D/2D fusion to the fluoroscopic image (Fig. 1A). ECoG contacts were manually marked on the fused images and visualized on the reconstructed cortical surface (Fig. 1B). Two bipolar signal pairs were used for the analysis: S1 (primary somatosensory, contact pair immediately posterior to the central sulcus,

spanning postcentral gyrus) and M1/PM (motor and premotor, contact pair immediately anterior to the central sulcus, spanning precentral gyrus).

Experimental protocol

ECoG recordings were obtained with a scalp ground and reference. Signal acquisition was performed using BCI2000 with g.USBamp 2 amplifiers (sampling rate: 2400 Hz, 0.1Hz–1000Hz bandpass filter). A data glove (5DT data glove 5 Ultra) monitored contralateral hand movement. Bipolar ECoG re-referencing was carried out for further analysis (Fig. 1). Each subject performed a block-design finger tapping task alternating 30 seconds blocks of rest (remaining as still as possible with eyes open) and left hand cued finger tapping (maximum amplitude with fastest comfortable speed). Two 30-second rest and movement blocks were analyzed for each subject. The first rest/movement block was recorded without GPi-stimulation (DBS-OFF state) while the second block was acquired with GPi-DBS stimulation (DBS-ON state, table 1). Experiments were conducted at least 15 minutes after intraoperative clinical testing to minimize the effects of stimulation on DBS-OFF state recordings.

Monopolar constant voltage stimulation (Fig. 1D, contact 1 (N= 8) or 2 (N=2) cathode, based on that providing the best intraoperative acute therapeutic response) with parameters similar to chronic therapy was used (with scalp (N=3) or shoulder (N=7) anode). Stimulation was applied using an analog neurostimulator (Medtronic model 3625). Prior to stimulation, clinical assessment of the patients' contralateral upper limb was performed by a movement disorders neurologist (author YB), including UPDRS Part III scores for tremor (item 3.17), rigidity (item 3.3) and bradykinesia (item 3.4). Clinical assessments were repeated with DBS-ON.

Data preprocessing

Signal analysis was performed using custom scripts in MATLAB (Mathworks, Natick, MA), Chronux toolbox [29] and Fieldtrip toolbox [30]. Data fragments containing electrical or movement artifact were excluded using previously described methods [31]. Data were band-pass filtered at 6–300 Hz using a two-way least squares FIR filter (*eegfilt.m*, forward and backward to ensure no phase distortion). Ambient line noise (60 Hz) and its harmonics were removed using the Fieldtrip toolbox's notch-filter. Stimulation-related artifacts were removed with a zero-phase Butterworth filter (order = 3, bandwidth = 4Hz). Filtering was done similarly for DBS-OFF and DBS-ON conditions and prior to segmentation of rest/movement blocks to minimize edge effects.

Power Spectral Density

Power spectral density (PSD) was calculated using the multitaper method [32] in 1-second consecutive time windows with no overlap for frequencies of 6 to 200 Hz with ±2 Hz frequency bandwidth (3 tapers). To account for variability in the baseline total power between contacts (single subject level) and subjects (group level), the total power was calculated as the integral of raw power values for frequencies 6–200 Hz (excluding frequencies removed due to line noise and stimulation artifact). Each PSD was then

normalized to the total rest (i.e., baseline) power. Average band power for frequency ranges of interest was then calculated from normalized spectra.

Phase-amplitude coupling

PAC was estimated using Tort's method of Modulation Index (MI) [33,34]. Parameters selected for PAC analysis were chosen based on previous critical analyses [35]. Briefly, signals were band-pass filtered using two-way least squares FIR filter (phase: 1–35 Hz, in 1 Hz steps and 2 Hz bandwidth; amplitude: 6–200 Hz in 2 Hz steps and bandwidth of double the phase-encoding frequency). Hilbert transform was then used to extract instantaneous phase and amplitude of the two components. Phase values were then binned (18 bins, 20° width) and mean amplitude distribution was calculated relative to the phase bins to create a phase-amplitude histogram. Kullback-Leibler divergence was used to measure deviation from a uniform distribution and derive MI values. To extract the preferred phase, the weights of the phase-amplitude histogram were used as amplitudes of a vector, with the center phase of each bin constituted the phase of the vector.

To evaluate the significance of derived MI values, for each frequency pair, we generated 1000 randomly generated versions of phase signal (using a random temporal shift in the phase signal relative to the amplitude signal) and calculated surrogate data. MI values were converted to Z-scores and the False Discovery Rate procedure was used with $q = 0.05$ to correct for multiple comparisons [36,37]. For each frequency pair with statistically significant PAC, the preferred phase of coupling was defined as the phase bin with maximal amplitude measurement. The circular mean of the preferred phase was calculated for all the frequency pairs in distinct frequency bands for each subject. Average PAC was calculated for distinct frequency band pairs (phase frequencies included β: 13–35 Hz, low β: 13–20 Hz and high β: 20–35 Hz and amplitude frequencies included γ (50–200 Hz)) and used for further statistical analyses across the population.

Statistical analysis

Statistical analysis was performed using SPSS (IBM Corp. Armonk, NY) and STATA (StataCorp LLC, College Station, TX). Statistically significant differences in spectral power between two conditions (movement/stimulation) at each frequency (6–200 Hz) were assessed using the two group test of the spectrum [38], with a null hypothesis that conditions have equal spectra within the cohort. The statistical properties of asymptotic distributions for power spectra are well known [38]. Our choice of the two-group test was based on the asymptotic probability distributions and jackknife correction of the difference z-scores. This method is advantageous as it corrects for the bias inherent to the spectral estimation process [26]. Since multitaper spectral analysis uses an orthogonal family of tapers (i.e., Slepian sequences) calculated using non-overlapping windows, the calculated tapered spectra can be reasonably assumed to be statistically independent. We derived the mean group spectra for each condition (across each cohort) along with the corresponding Z statistics using asymptotic spectral probability distribution. The 95% confidence intervals were then calculated based on the Jackknife estimation of variance as previously described [38]. To address the issue of multiple comparisons, we note that differences in spectra due to the chance are likely to be present at discrete frequencies, while neurophysiological differences

span contiguous frequency ranges (e.g., α, β). Since spectral estimates at frequencies separated by less than the bandwidth of the multitaper method (4 Hz) are inherently correlated, we rejected the null hypothesis for all candidate frequencies constituting bands whose width is larger than 4 Hz [38,39].

Another complementary method was used to assess the statistical significance of power changes. The average band power values were calculated for the different frequency bands α, low β, high β, and γ. Because our sample size is <50, the Shapiro-Wilk test was used to assess normality of distribution prior to comparing power (at different frequency bands) and PAC. Since the normality condition was not satisfied, non-parametric paired sample Wilcoxon signed-rank test was used to compare power and PAC across cortical contacts and conditions. Linear correlations with clinical scores were evaluated with non-parametric Spearman correlation and corresponding p-values with a statistical significance level of 0.05. All resulting p-values were corrected for multiple comparisons using Bonferroni or Holm's sequential Bonferroni method [40].

Linear mixed-effect model (LMEM) was used to examine the difference in the average spectral power and PAC, between rest/movement states with DBS-OFF/ON at each recording sites for the two frequency bands of interest. LMEM is a regression method that models the linear relationship between a response variable and independent variables, with coefficients that vary with respect to grouping variables [41]. In this study, each subject contributed multiple samples in a repeated measures design. LMEM, unlike analysis of variance based techniques (i.e. ANOVA), is a robust statistical technique for repeated measures study design and accounts for the inherent correlation between repeated measures from each subject [42]. LMEMs were constructed with four two-level grouping factors including stimulation state (DBS-OFF and DBS-ON), movement state (rest and movement), and frequency band (Low and High β) and recording sites (S1 and M1/PM). The average values of the log-transformed power, and PAC z-scores as a function of the four grouping variables were used as response variables. Interactions between effects were studied as part of the model and studied for significance ($P<0.05$) and corrected for multiple comparisons using Bonferroni method.

Results

M1/PM has greater high β power and high β-γ PAC than S1

Initially, we compared frequency-specific power S1 and M1/PM at rest with DBS-OFF (Fig. 2A–B). The two group test of spectra revealed that S1 had significantly greater power for frequencies between 8 and 13 Hz (α frequencies) and M1/PM had significantly larger power for frequencies between 19 and 39 Hz (high β frequencies, Fig. 2A). Differences were confirmed using paired Wilcoxon signed-rank test and band power: α band power was significantly larger at S1 contact ($P=0.03$) whereas high β power was significantly larger at M1/PM ($P=0.038$).

Similarly, we compared S1 and M1/PM PAC at rest with DBS-OFF (Fig. 2C). Z-score PAC maps were averaged across the low and high β phase encoding frequencies and γ for amplitude encoding frequencies for each cortical region per subject (Fig. 2C dotted boxes).

M1/PM exhibited higher PAC for both low and high β phase encoding frequencies compared to S1, where PAC was only minimally evident (Fig. 2C). Only high β PAC was found to be significantly different (P=0.014, corrected Wilcoxon signed rank test; P=0.1, for low β PAC, Fig. 2D). Average cortical PAC was maximal at M1/PM at a phase encoding frequency of 23 ±1.46 Hz and amplitude frequency of 106 ±25.67 Hz. Corresponding values for S1 were 23.7±2.38 Hz and 101±34.46 Hz, respectively.

Movement modulates low β power and β-γ PAC in sensorimotor cortices

With DBS-OFF, contralateral finger tapping significantly suppressed S1 and M1/PM spectral power in the 9–13 Hz and 9–18 Hz ranges, respectively (Fig. 3A). Movement-related power increases were noted between 28 and 200 Hz in both sensorimotor cortical signals (two group test of spectra, Fig. 3A). Similar results were observed with Wilcoxon signed-rank test of band power, with significant power suppression of α at S1 (P=0.025) and M1/PM (P=0.008). Changes in average low β power were only significant in M1/PM (P=0.008). High β power was not significantly modulated at either location (P=0.6 and 0.6, for S1 and M1/PM respectively). Contralateral hand movement likewise resulted in significant power increase in γ frequencies (P=0.025 and 0.008, for S1 and M1/PM respectively, Fig. 3B). LMEM revealed a significant interaction between frequency band (low vs high β) and condition (rest vs movement) in the DBS-OFF state (χ^2=6.47, P=0.022, corrected), confirming that low and high β power are differentially modulated by movement (main effects: rest/movement condition: χ^2=5.22, P=0.04, frequency band (low vs high β): χ^2=19.09, P<0.001).

Contralateral hand movement also reduced sensorimotor cortical low/high β-γ PAC (Fig. 3C–D). Only changes in high β phase encoded PAC at M1/PM were significant (P=0.028, Wilcoxon signed-rank test) whereas high β phase encoded PAC at S1 were unchanged (P=0.16, corrected). Moreover, movement-related suppression of PAC was not significant for low β encoding frequencies (P=0.09 and 0.3, corrected for S1 and M1/PM, respectively). LMEM showed a significant main effect of movement on PAC (rest vs movement, χ^2=10.13, P=0.003, corrected). However, no significant effect was found for the frequency of phase encoding (low vs high β, χ^2=0.39, P=0.54, corrected) or for the interaction between movement condition and phase encoding frequency (χ^2=0.19, P=0.76, corrected).

Average phase and amplitude encoding frequencies for β-γ PAC during movement with DBS-OFF were phase: 22±1.76 Hz, amplitude: 111.6±18 Hz and phase: 25±1.68 Hz, amplitude: 109.6±19.57 Hz for S1 and M1/PM, respectively. The movement did not significantly alter the phase/amplitude encoding frequencies (P>0.05, Wilcoxon signed-rank test).

Acute GPi-DBS modulates sensorimotor cortical high β-γ PAC without modulating spectral power

Acute GPi-DBS significantly improved clinical scores (P=0.02 for rigidity and P=0.01 for bradykinesia, Table 1). GPi-DBS did not significantly modulate sensorimotor cortical spectral power in either the rest (Fig. 4A) or movement (Fig. 5A) conditions (two group test of spectra). Nonparametric Wilcoxon signed-rank test of predefined frequency bands

confirmed no significant changes in α, low/high β or γ frequencies across the sensorimotor cortices with GPi-DBS (Fig. 4B, 5B).

Despite a lack of effect on spectral power, GPi-DBS suppressed cortical PAC at S1 and M1/PM during both rest (Fig. 4C–D) and movement conditions (Fig. 5C–D), although only significant at M1/PM during both rest (P=0.008, corrected) and movement (P=0.04, corrected, Wilcoxon signed-rank test). We used LMEM to confirm the overall effect of stimulation on cortical PAC and investigate interactions between frequency band and stimulation state. The overall main effect for stimulation state was significant (χ^2=7.55, P=0.006). However, there was no main effect of the frequency band (irrespective of movement state, χ^2=0.01, P=0.97) and there was no significant interaction between stimulation state and frequency band (χ^2=0.7, P=0.4).

During rest with DBS-ON, the average frequencies of maximal coupling were phase: 23.1±2.01Hz and amplitude: 119.6±18.4 Hz for S1 and phase: 24.2±1.5 Hz, amplitude: 102.6±18.72 Hz for M1/PM. Average phase/amplitude encoding frequencies of maximal coupling did not change between DBS states (ON vs OFF) at any of the cortical sites examined (Wilcoxon signed rank test, P>0.05), suggesting that GPi-DBS reduces the magnitude of PAC without changing the preferred frequencies for maximal coupling.

To ensure these results were not driven by the order of experiments, we compared resting cortical PAC in a subgroup of subjects (N=8) for whom we obtained additional resting state recordings after termination of stimulation. Such comparison revealed no significant difference in the PAC, for low or high β phase encoding frequencies, at either cortical contact (P>0.1, Wilcoxon signed-rank, Fig. 6) before and after cessation of stimulation.

Modeling the effects of hand movement and GPi-DBS on sensorimotor physiology

LMEM analysis of average spectral β band power as a full-factor combination of movement condition (rest vs movement), stimulation state (ON vs OFF), the frequency band (low vs high β) and location (S1 or M1/PM) was statistically significant (χ^2=133.22, P<0.0001). Tests for the effect of main factors in the model identified the movement condition (χ^2 =19.96, P<0.0001) and frequency band (χ^2=43.1, P<0.0001) but not the stimulation state (χ^2=1.19, P=0.275) as significant factors. There was no significant interaction between movement condition and stimulation state on sensorimotor spectral power (χ^2=1.55, P=0.212). However the interaction between movement condition and frequency band was significant: (χ2= 12.48, P=0.0004) further confirming that regardless of the stimulation state, movement affected beta sub-bands differently.

Similar LMEM analysis with cortical PAC modeled using the grouping variables described above was also significant (χ^2=71.53, P<0.0001). Tests for overall effects identified movement condition (χ^2= 13.99, P=0.0002) and stimulation state (χ^2=7.55, P=0.006) as main factors that significantly modulated cortical PAC. The interaction between the two main factors examined, however, was not found to be statistically significant (χ^2=0.58, P=0.44). As a result, we could not reject the null hypothesis that contralateral hand movement and DBS change cortical PAC in different ways.

Motor cortical high β-γ PAC correlates with bradykinesia and changes in proportion to therapeutic improvements with GPi-DBS

We investigated the correlation between each disease symptom (i.e. tremor, rigidity and bradykinesia) in the "untreated" state (DBS-OFF) and low/high β corresponding power and PAC values during rest. DBS-OFF UPDRS measurements were not available for one subject (P3), therefore this analysis was performed excluding P3 (N=9). Power (low or high β) did not correlate with any clinical scores examined. However, there was a significant and positive correlation between cortical high β-γ PAC at M1/PM and bradykinesia scores (Fig. 7A, Spearman correlation, Rho=0.59, P=0.045).

Based on this finding, we further investigated whether the degree of DBS-related suppression of high β-γ PAC was related to the clinical improvement in bradykinesia. We regressed the difference in the PAC against the difference in clinical scores (DBS-OFF minus DBS-ON) using non-parametric Spearman correlation. GPi-DBS related suppression of high β-γ PAC at M1/PM significantly correlated with improvements in bradykinesia (Rho = 0.61, P=0.04, Fig. 7B). None of the low/high β power values nor low β-γ PAC correlated with baseline disease severity nor improvement in clinical scores (P>0.1, Wilcoxon signed-rank test).

Discussion

Excessive β oscillations throughout the different nodes of BGTC network have been linked to the symptomatology of PD [1–8,43–46]. In the untreated state, STN β power is shown to correlate with the severity of rigidity and bradykinesia, and decrease in proportion to clinical improvement with therapy [1,3,4,46]. Thus, STN β power appears to be a promising disease biomarker to target including its potential for driving adaptive/closed-loop DBS systems for PD [47–50]. More recently, de Hemptinne and colleagues showed that β-γ PAC at motor cortex is exaggerated in PD subjects [14]. They further showed that β-γ PAC, but not cortical β power, is modulated by STN-DBS [17], concluding that the therapeutic effect of STN-DBS is reflected in attenuations in the excessive cortical coupling. STN-DBS has subsequently been shown to not only modulate local subthalamic β power but also suppresses STN-motor cortical β coherence [8].

Our current findings show that therapeutic stimulation of the GPi also results in the attenuation of motor cortical PAC, but not cortical β power, similar to STN-DBS [17]. Given that both the STN and GPi are clinically efficacious therapeutic targets in managing PD symptoms [21], our present findings suggest that DBS at either target may produce its therapeutic effect by regularizing excessive motor cortical PAC but that it is not necessarily mediated (at least not exclusively) by the hyperdirect pathway. It is possible that GPi- and STN-DBS therapeutic effects are mediated through different pathways (motor thalamus vs hyperdirect pathway). Conversely, STN DBS may be mediated through the GPi and motor thalamus [17]. The alteration of higher-order cross-frequency interactions (in the form of PAC), independent of power modulation, indicates that PAC modulation is not a byproduct of changes to the power of the underlying phase encoding frequencies. We propose that higher-order oscillatory interactions (be it locally in the form of PAC or inter-regionally in terms of coherence) may reflect PD pathophysiology more closely than exaggerated local

oscillatory power [8,51,52]. Moreover, because cortical β power modulation was observed only with contralateral hand movement, simultaneous assessment of both cortical β power and β-γ PAC may provide a useful tool for differentiating movement-related vs therapy-related changes in cortical physiology.

New studies suggest exaggerated motor cortical PAC in PD may be related to the sharpness of β oscillations and that DBS normalizes PAC by modifying waveform shape (i.e. flattening β oscillations) by decrementing the synchrony of synaptic input to M1 [53,54]. Our finding of similar effects of GPi-DBS and STN-DBS in normalizing motor cortical PAC, given distinct anatomical connectivity of the two targets further indicates that therapy exerts its effect by regularizing the synchronous input to the motor cortex by reducing exaggerated beta hypersynchrony in the BGTC network.

A second main finding in this study is that both movement and GPi-DBS attenuation of M1/PM PAC favor the high β range whereas movement in the absence of GPi-DBS results in a significant attenuation of low but not high β oscillatory power in the sensorimotor cortices. This dissociation between effects of movement and GPi-DBS on the modulation of cortical β sub-bands suggests that high and low β frequencies may mediate distinct functional roles where cortical low β power is related to the normal motor control and high β underlies the hypersynchronized state related to PD motor symptomology. Moreover, studies of hemiparkinsonian animals showed that with motor activity, low β power was reduced but high β activity was increased in the motor cortex in the dopamine-depleted hemisphere [55–57]. High β activity was most pronounced when the animals were engaged in the ongoing motor activity and significantly reduced with L-Dopa administration. A recent study reported that modulation of low β pallidocortical coherence may be also important for normal motor control [58].

Non-linear correlations between low and high β oscillations have been reported in PD subjects during the off medication state [59]. Levodopa administration significantly decreases these correlations and increases segregation between these two β bands [59]. In the basal ganglia, these patients show clinical improvement with pharmacologic and DBS therapy corresponded with a reduction in local low β power in the STN while cortico-STN coupling within the high β range is most responsive to therapeutic interventions [8,45,60,61] The dissociation of higher-order oscillatory interactions (such as PAC) in terms of low and high β frequencies suggests that motor cortical PAC can similarly be separated into distinct functional domains. Our results demonstrate that only motor cortical PAC at high β frequencies positively correlated with bradykinesia scores and is significantly suppressed by GPi-DBS. On the other hand, cortical low β power changes in response to contralateral body movement and not stimulation. These findings along with previous reports on the suppression of subthalamic low β power with treatment [8] further support a functional dissociation of β sub-bands within and across cortical and subcortical structures within the motor network.

The coupling between STN and motor cortex in low vs high β band has been suggested to reflect distinct contributions of indirect vs hyperdirect pathways, respectively [8]. To maintain this perspective, one would assume that GPi-DBS blocks high β signals that

propagate via the hyperdirect BGTC loop. However, we have observed high β even in GPe [20], suggesting that high β in fact reverberates throughout the entire BGTC circuit and is not specific to the hyperdirect pathway. Given distinct oscillatory bands function as unique communication channels across distant nodes in brain networks [62], we propose it is more likely that distinct spectral bands relate to unique functions rather than structurally segregated anatomic pathways [63].

Limitations

We acknowledge that our study is limited by the relatively small number of PD subjects included (N=10) and that no control group was included due to inherent challenges of intraoperative recording. However, our coherent findings suggest that these results could be extended to the larger population.

Conclusions

Excessive high β-γ PAC may be a more informative biomarker for PD disease state [15] and suited for driving closed-loop DBS systems than β oscillatory power alone, regardless of DBS target. The correlation of high β-γ PAC with both stimulation state and symptoms further indicate its suitability as a potential marker of therapeutic state.

Acknowledgments

Funding

This work was supported by the National Institutes of Biomedical Imaging and Bioengineering [K23 EB014326], National Institutes of Neurological Disorders and Stroke [R01NS097782] and philanthropic support from Casa Colina Centers for Rehabilitation. NA was supported by National Insitute of neurological disorders and stroke [R25-NS079198]. MM also was supported by postdoctoral fellowship from American Parkinson Disease Association (APDA, NY).

Authors would like to thank all the patients consented to participate in this study without whom recording of brain electrophysiology was not possible.

Abbreviations

BGTC	Basal ganglia-thalamo-cortical
DBS	Deep brain stimulation
ECoG	Electrocorticography
GPi	Globus pallidus internus
HFO	High frequency oscillations
LFP	Local field potentials
LMEM	Linear Mixed Effect Modeling
MER	Microelectrode recording
PD	Parkinson disease

PAC	Phase amplitude coupling
PSD	Power spectral density
STN	Subthalamic nucleus
UPDRS	Unified Parkinson disease rating scale

References

1. Levy R, Ashby P, Hutchison WD, Lang AE, Lozano AM, Dostrovsky JO. Dependence of subthalamic nucleus oscillations on movement and dopamine in Parkinson's disease. Brain. 2002; 125:1196–209. [PubMed: 12023310]
2. Stoffers D, Bosboom JLW, Wolters ECEc, Stam CJ, Berendse HW. Dopaminergic modulation of cortico-cortical functional connectivity in Parkinson's disease: an MEG study. Exp Neurol. 2008; 213:191–5. DOI: 10.1016/j.expneurol.2008.05.021 [PubMed: 18590728]
3. Chen CC, Hsu YT, Chan HL, Chiou SM, Tu PH, Lee ST, et al. Complexity of subthalamic 13–35 Hz oscillatory activity directly correlates with clinical impairment in patients with Parkinson's disease. Exp Neurol. 2010; 224:234–40. DOI: 10.1016/j.expneurol.2010.03.015 [PubMed: 20353774]
4. Eusebio, a, Thevathasan, W., Doyle Gaynor, L., Pogosyan, a, Bye, E., Foltynie, T., et al. Deep brain stimulation can suppress pathological synchronisation in parkinsonian patients. J Neurol Neurosurg Psychiatry. 2011; :82.doi: 10.1136/jnnp.2010.217489
5. Crowell AL, Ryapolova-Webb ES, Ostrem JL, Galifianakis NB, Shimamoto S, Lim DA, et al. Oscillations in sensorimotor cortex in movement disorders: an electrocorticography study. Brain. 2012; 135:615–30. DOI: 10.1093/brain/awr332 [PubMed: 22252995]
6. Marreiros AC, Cagnan H, Moran RJ, Friston KJ, Brown P. Basal ganglia-cortical interactions in Parkinsonian patients. Neuroimage. 2013; 66:301–10. DOI: 10.1016/j.neuroimage.2012.10.088 [PubMed: 23153964]
7. Stein E, Bar-Gad I. beta oscillations in the cortico-basal ganglia loop during parkinsonism. Exp Neurol. 2013; 245:52–9. DOI: 10.1016/j.expneurol.2012.07.023 [PubMed: 22921537]
8. Oswal A, Beudel M, Zrinzo L, Limousin P, Hariz M, Foltynie T, et al. Deep brain stimulation modulates synchrony within spatially and spectrally distinct resting state networks in Parkinson's disease. Brain. 2016; 139:1482–96. DOI: 10.1093/brain/aww048 [PubMed: 27017189]
9. Dorval AD, Russo GS, Hashimoto T, Xu W, Grill WM, Vitek JL. Deep brain stimulation reduces neuronal entropy in the MPTP-primate model of Parkinson's disease. J Neurophysiol. 2008; 100:2807–18. DOI: 10.1152/jn.90763.2008 [PubMed: 18784271]
10. Dorval AD, Grill WM. Deep brain stimulation of the subthalamic nucleus reestablishes neuronal information transmission in the 6-OHDA rat model of parkinsonism. J Neurophysiol. 2014; 111:1949–59. DOI: 10.1152/jn.00713.2013 [PubMed: 24554786]
11. Darbin O, Dees D, Martino A, Adams E, Naritoku D. An entropy-based model for basal ganglia dysfunctions in movement disorders. Biomed Res Int. 2013; 2013:742671.doi: 10.1155/2013/742671 [PubMed: 23762856]
12. Dorval AD, Kuncel AM, Birdno MJ, Turner Da, Grill WM. Deep brain stimulation alleviates parkinsonian bradykinesia by regularizing pallidal activity. J Neurophysiol. 2010; 104:911–21. DOI: 10.1152/jn.00103.2010 [PubMed: 20505125]
13. Anderson CJ, Sheppard DT, Huynh R, Anderson DN, Polar CA, Dorval AD. Subthalamic deep brain stimulation reduces pathological information transmission to the thalamus in a rat model of parkinsonism. Front Neural Circuits. 2015; 9:31.doi: 10.3389/fncir.2015.00031 [PubMed: 26217192]
14. de Hemptinne C, Ryapolova-Webb ES, Air EL, Garcia PA, Miller KJ, Ojemann JG, et al. Exaggerated phase-amplitude coupling in the primary motor cortex in Parkinson disease. Proc Natl Acad Sci U S A. 2013; 110:4780–5. DOI: 10.1073/pnas.1214546110 [PubMed: 23471992]

15. Kondylis ED, Randazzo MJ, Alhourani A, Lipski WJ, Wozny TA, Pandya Y, et al. Movement-related dynamics of cortical oscillations in Parkinson's disease and essential tremor. Brain. 2016; 139:2211–23. DOI: 10.1093/brain/aww144 [PubMed: 27329771]
16. Swann NC, de Hemptinne C, Aron AR, Ostrem JL, Knight RT, Starr PA. Elevated synchrony in Parkinson disease detected with electroencephalography. Ann Neurol. 2015; 78:742–50. DOI: 10.1002/ana.24507 [PubMed: 26290353]
17. de Hemptinne C, Swann NC, Ostrem JL, Ryapolova-Webb ES, San Luciano M, Galifianakis NB, et al. Therapeutic deep brain stimulation reduces cortical phase-amplitude coupling in Parkinson's disease. Nat Neurosci. 2015; 18:779–86. DOI: 10.1038/nn.3997 [PubMed: 25867121]
18. van Wijk BCM, Beudel M, Jha A, Oswal A, Foltynie T, Hariz MI, et al. Subthalamic nucleus phase-amplitude coupling correlates with motor impairment in Parkinson's disease. Clin Neurophysiol. 2016; 127:2010–9. [PubMed: 26971483]
19. Litvak V, Jha A, Eusebio A, Oostenveld R, Foltynie T, Limousin P, et al. Resting oscillatory cortico-subthalamic connectivity in patients with Parkinson's disease. Brain. 2011; 134:359–74. DOI: 10.1093/brain/awq332 [PubMed: 21147836]
20. Tsiokos C, Malekmohammadi M, Au Yong N, Pouratian N. Pallidal low β-low γ phase-amplitude coupling inversely correlates with Parkinson disease symptoms. Clin Neurophysiol. 2017; doi: 10.1016/j.clinph.2017.08.001
21. Mansouri A, Taslimi S, Badhiwala JH, Witiw CD, Nassiri F, Odekerken VJJ, et al. Deep brain stimulation for Parkinson's disease: meta-analysis of results of randomized trials at varying lengths of follow-up. J Neurosurg. 2017; :1–15. DOI: 10.3171/2016.11.JNS16715
22. Follett KA, Weaver FM, Stern M, Hur K, Harris CL, Luo P, et al. Pallidal versus subthalamic deep-brain stimulation for Parkinson's disease. N Engl J Med. 2010; 362:2077–91. DOI: 10.1056/NEJMoa0907083 [PubMed: 20519680]
23. Williams NR, Foote KD, Okun MS. STN vs. GPi Deep Brain Stimulation: Translating the Rematch into Clinical Practice. Mov Disord Clin Pract. 2014; 1:24–35. DOI: 10.1002/mdc3.12004 [PubMed: 24779023]
24. Nambu A, Tokuno H, Takada M. Functional significance of the cortico-subthalamo-pallidal "hyperdirect" pathway. Neurosci Res. 2002; 43:111–7. DOI: 10.1016/S0168-0102(02)00027-5 [PubMed: 12067746]
25. Randazzo MJ, Kondylis ED, Alhourani A, Wozny TA, Lipski WJ, Crammond DJ, et al. Three-dimensional localization of cortical electrodes in deep brain stimulation surgery from intraoperative fluoroscopy. Neuroimage. 2016; 125:515–21. DOI: 10.1016/j.neuroimage.2015.10.076 [PubMed: 26520771]
26. Malekmohammadi M, AuYong N, Price CM, Tsolaki E, Hudson AE, Pouratian N. Propofol-induced Changes in alpha-beta sensorimotor cortical connectivity. Anesthesiology. 2017; :1.doi: 10.1097/ALN.0000000000001940
27. Dale AM, Fischl B, Sereno MI. Cortical surface-based analysis. I. Segmentation and surface reconstruction. Neuroimage. 1999; 9:179–94. DOI: 10.1006/nimg.1998.0395 [PubMed: 9931268]
28. Ratib O, Rosset A. Open-source software in medical imaging: Development of OsiriX. Int J Comput Assist Radiol Surg. 2006; 1:187–96. DOI: 10.1007/s11548-006-0056-2
29. Bokil H, Andrews P, Kulkarni JE, Mehta S, Mitra PP. Chronux: a platform for analyzing neural signals. J Neurosci Methods. 2010; 192:146–51. DOI: 10.1016/j.jneumeth.2010.06.020 [PubMed: 20637804]
30. Oostenveld R, Fries P, Maris E, Schoffelen J-M, Oostenveld R, Fries P, et al. FieldTrip: Open Source Software for Advanced Analysis of MEG, EEG, and Invasive Electrophysiological Data, FieldTrip: Open Source Software for Advanced Analysis of MEG, EEG, and Invasive Electrophysiological Data. Comput Intell Neurosci Comput Intell Neurosci. 2010; 2011:2011, e156869.doi: 10.1155/2011/156869
31. Tsiokos C, Hu X, Pouratian N. 200–300Hz movement modulated oscillations in the internal globus pallidus of patients with Parkinson's Disease. Neurobiol Dis. 2013; 54:464–74. DOI: 10.1016/j.nbd.2013.01.020 [PubMed: 23388190]
32. Thomson DJ. Spectrum estimation and harmonic analysis. Proc IEEE. 1982; 70:1055–96. DOI: 10.1109/PROC.1982.12433

33. Tort ABL, Komorowski R, Eichenbaum H, Kopell N. Measuring phase-amplitude coupling between neuronal oscillations of different frequencies. J Neurophysiol. 2010; 104:1195–210. DOI: 10.1152/jn.00106.2010 [PubMed: 20463205]
34. Malekmohammadi M, Elias WJ, Pouratian N. Human thalamus regulates cortical activity via spatially specific and structurally constrained phase-amplitude coupling. Cereb Cortex. 2015; : 25.doi: 10.1093/cercor/bht358
35. Aru JJ, Aru JJ, Priesemann V, Wibral M, Lana L, Pipa G, et al. Untangling cross-frequency coupling in neuroscience. Curr Opin Neurobiol. 2015; 31:51–61. DOI: 10.1016/j.conb.2014.08.002 [PubMed: 25212583]
36. Benjamini Y, Drai D, Elmer G, Kafkafi N, Golani I. Controlling the false discovery rate in behavior genetics research. Behav Brain Res. 2001; 125:279–84. [PubMed: 11682119]
37. Genovese CR, Lazar NA, Nichols T. Thresholding of statistical maps in functional neuroimaging using the false discovery rate. Neuroimage. 2002; 15:870–8. DOI: 10.1006/nimg.2001.1037 [PubMed: 11906227]
38. Bokil H, Purpura K, Schoffelen JM, Thomson D, Mitra P. Comparing spectra and coherences for groups of unequal size. J Neurosci Methods. 2007; 159:337–45. DOI: 10.1016/j.jneumeth.2006.07.011 [PubMed: 16945422]
39. Goldfine AM, Victor JD, Conte MM, Bardin JC, Schiff ND. Determination of awareness in patients with severe brain injury using EEG power spectral analysis. 2011; doi: 10.1016/j.clinph.2011.03.022
40. Holm S. A simple sequential rejective multiple test procedure. Scand J Stat. 1979; 6:65–70.
41. Gelman, A., Hill, J. Data analysis using regression and multilevel/hierarchical models. Cambridge University Press; 2007.
42. Wainwright PE, Leatherdale ST, Dubin JA. Advantages of mixed effects models over traditional ANOVA models in developmental studies: A worked example in a mouse model of fetal alcohol syndrome. Dev Psychobiol. 2007; 49:664–74. DOI: 10.1002/dev.20245 [PubMed: 17943976]
43. Brittain J-SS, Brown P. Oscillations and the basal ganglia: motor control and beyond. Neuroimage. 2014; 85(Pt 2):637–47. DOI: 10.1016/j.neuroimage.2013.05.084 [PubMed: 23711535]
44. Eusebio A, Brown P. Oscillatory activity in the basal ganglia. Park Relat Disord. 2007; 13:S434–6. DOI: 10.1016/S1353-8020(08)70044-0
45. Oswal A, Brown P, Litvak V. Synchronized neural oscillations and the pathophysiology of Parkinson's disease. Curr Opin Neurol. 2013; 26:662–70. DOI: 10.1097/WCO.0000000000000034 [PubMed: 24150222]
46. Kuhn AA, Tsui A, Aziz T, Ray N, Brucke C, Kupsch A, et al. Pathological synchronisation in the subthalamic nucleus of patients with Parkinson's disease relates to both bradykinesia and rigidity. Exp Neurol. 2009; 215:380–7. DOI: 10.1016/j.expneurol.2008.11.008 [PubMed: 19070616]
47. Little S, Brown P. The functional role of beta oscillations in Parkinson's disease. Park Relat Disord. 2014; 20(Suppl 1):S44–8. DOI: 10.1016/S1353-8020(13)70013-0
48. Little S, Brown P. What brain signals are suitable for feedback control of deep brain stimulation in Parkinson's disease? Ann N Y Acad Sci. 2012; 1265:9–24. DOI: 10.1111/j.1749-6632.2012.06650.x [PubMed: 22830645]
49. Little S, Beudel M, Zrinzo L, Foltynie T, Limousin P, Hariz M, et al. Bilateral adaptive deep brain stimulation is effective in Parkinson's disease. J Neurol Neurosurg Psychiatry. 2015; doi: 10.1136/jnnp-2015-310972
50. Little S, Pogosyan A, Neal S, Zavala B, Zrinzo L, Hariz M, et al. Adaptive deep brain stimulation in advanced Parkinson disease. Ann Neurol. 2013; 74:449–57. DOI: 10.1002/ana.23951 [PubMed: 23852650]
51. Weiss D, Klotz R, Govindan RB, Scholten M, Naros G, Ramos-Murguialday A, et al. Subthalamic stimulation modulates cortical motor network activity and synchronization in Parkinson's disease. Brain. 2015; 138:679–93. DOI: 10.1093/brain/awu380 [PubMed: 25558877]
52. Alhourani A, McDowell MM, Randazzo MJ, Wozny TA, Kondylis ED, Lipski WJ, et al. Network effects of deep brain stimulation. J Neurophysiol. 2015; 114:2105–17. DOI: 10.1152/jn.00275.2015 [PubMed: 26269552]

53. Cole SR, Voytek B. Brain Oscillations and the Importance of Waveform Shape. Trends Cogn Sci. 2017; 21:137–49. DOI: 10.1016/j.tics.2016.12.008 [PubMed: 28063662]
54. Cole SR, van der Meij R, Peterson EJ, de Hemptinne C, Starr PA, Voytek B. Nonsinusoidal Beta Oscillations Reflect Cortical Pathophysiology in Parkinson's Disease. J Neurosci. 2017; 37:4830–40. DOI: 10.1523/JNEUROSCI.2208-16.2017 [PubMed: 28416595]
55. Delaville C, Cruz AV, McCoy AJ, Brazhnik E, Avila I, Novikov N, et al. Oscillatory activity in basal ganglia and motor cortex in an awake behaving rodent model of Parkinson's disease. Basal Ganglia. 2014; 3:221–7. DOI: 10.1016/j.baga.2013.12.001 [PubMed: 25667820]
56. Brazhnik E, Novikov N, McCoy AJ, Cruz AV, Walters JR. Functional correlates of exaggerated oscillatory activity in basal ganglia output in hemiparkinsonian rats. Exp Neurol. 2014; 261:563–77. DOI: 10.1016/j.expneurol.2014.07.010 [PubMed: 25084518]
57. Avila I, Parr-Brownlie LC, Brazhnik E, Castañeda E, Bergstrom DA, Walters JR. Beta frequency synchronization in basal ganglia output during rest and walk in a hemiparkinsonian rat. Exp Neurol. 2010; 221:307–19. DOI: 10.1016/j.expneurol.2009.11.016 [PubMed: 19948166]
58. van Wijk BCM, Neumann W-J, Schneider G-H, Sander TH, Litvak V, Kühn AA. Low-beta cortico-pallidal coherence decreases during movement and correlates with overall reaction time. Neuroimage. 2017; doi: 10.1016/j.neuroimage.2017.07.024
59. Marceglia S, Bianchi AM, Baselli G, Foffani G, Cogiamanian F, Modugno N, et al. Interaction between rhythms in the human basal ganglia: Application of bispectral analysis to local field potentials. IEEE Trans Neural Syst Rehabil Eng. 2007; 15:483–92. [PubMed: 18198705]
60. Lopez-Azcarate J, Tainta M, Rodriguez-Oroz MC, Valencia M, Gonzalez R, Guridi J, et al. Coupling between beta and high-frequency activity in the human subthalamic nucleus may be a pathophysiological mechanism in Parkinson's disease. J Neurosci. 2010; 30:6667–77. DOI: 10.1523/JNEUROSCI.5459-09.2010 [PubMed: 20463229]
61. Priori A, Foffani G, Pesenti A, Tamma F, Bianchi AM, Pellegrini M, et al. Rhythm-specific pharmacological modulation of subthalamic activity in Parkinson's disease. Exp Neurol. 2004; 189:369–79. DOI: 10.1016/j.expneurol.2004.06.001 [PubMed: 15380487]
62. Fries P. A mechanism for cognitive dynamics: neuronal communication through neuronal coherence. Trends Cogn Sci. 2005; 9:474–80. DOI: 10.1016/j.tics.2005.08.011 [PubMed: 16150631]
63. Sharott A, Gulberti A, Hamel W, Köppen JA, Münchau A, Buhmann C, et al. Spatio-temporal dynamics of cortical drive to human subthalamic nucleus neurons in Parkinson's disease. Neurobiol Dis. 2018; doi: 10.1016/J.NBD.2018.01.001

Highlights

1. GPi-DBS modulates motor cortical signals similar to the STN-DBS
2. Movement suppresses low β power and high β-γ PAC in motor cortex
3. GPi-DBS suppresses motor cortical high β-γ PAC without changes in cortical β power
4. Motor cortical high β-γ PAC correlates with the severity of bradykinesia
5. GPi-DBS reduces high β-γ PAC proportionally to the improvement in bradykinesia

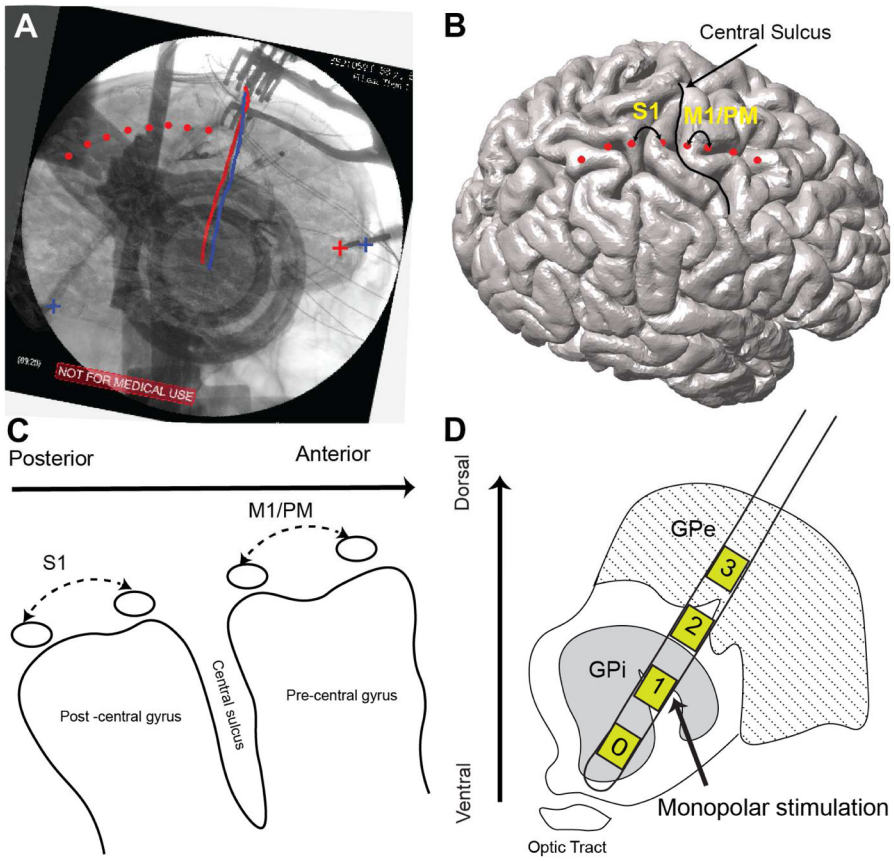

Figure 1.

Localization of cortical ECoG strip and cortical signals used for analysis (A) registration of pre-operative structural high resolution T1 weighted MRI and CT to co-localize cortical brain surface and skull. Tips of stereotactic frame and DBS leads (marked by + signs and straight red and blue lines on the image, respectively) are used as landmark to complete 2D–3D fusion of fluoroscopic image and cortical surface. One the fusion is complete cortical contacts (visible on the fluoroscopic image) are marked manually on the fused images. (B) Marked ECoG contacts are illustrated on the cortical surface and relative to central sulcus. (C) Two cortical bipolar signals spanning post to pre central gyri (S1 and M1/PM) are marked and used for all of the analyses. (D) DBS lead (Medtronic model 3387) penetrating through pallidum. Monopolar channel 1 or 2 was used to deliver high frequency stimulation. (For more detailed description of the registration method please refer to the online supplementary material)

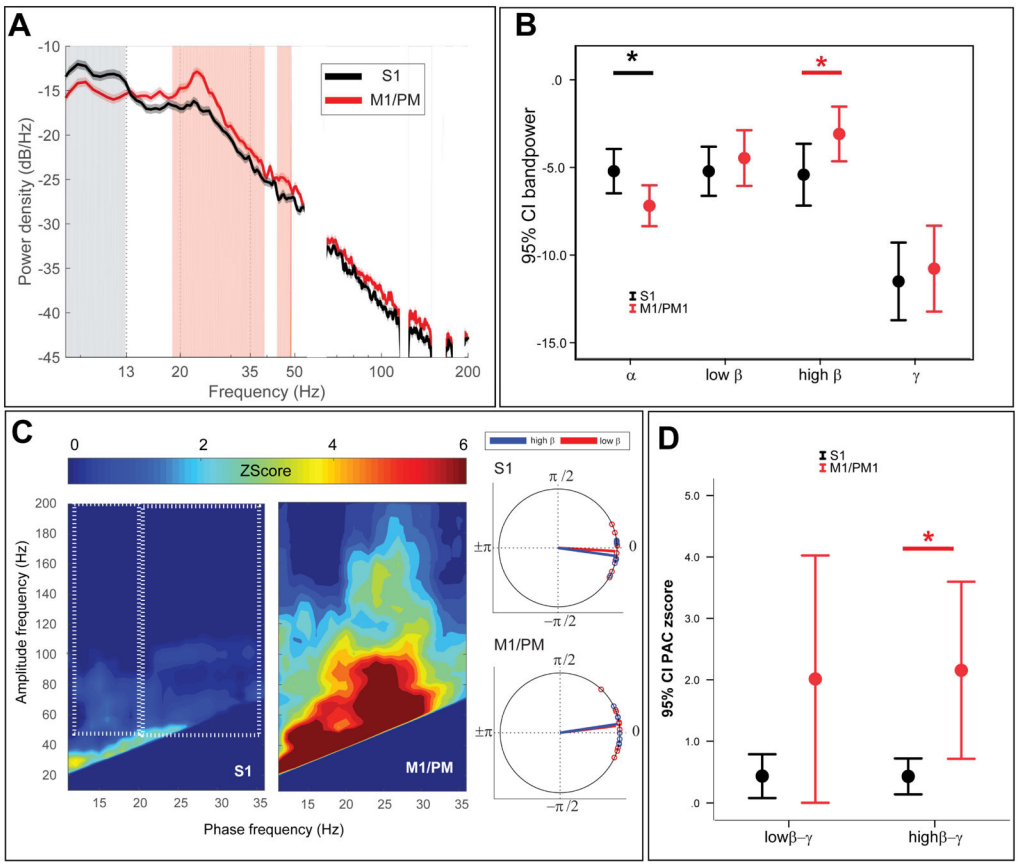

Figure 2.

Comparison of spectral power and PAC between S1 and M1/PM (A) Group average PSDs are plotted for S1 (green trace) and M1/PM (red trace). Vertical shade represents statistically significant difference observed by two-group test of spectrum. Frequency axis is plotted in log format to magnify changes in β band. (B) Average band power values are also compared between S1 (green) and M1/PM (red). Asterisk (*) sign indicates statistically significant difference ($P<0.05$, tested by non-parametric Wilcoxon signed-rank test, corrected for multiple comparisons using Bonferroni). Each bar shows the mean (across the cohort) and 95% confidence interval of the mean. (C) On the left hand side, average z-score maps for the cohort are represented, white dotted rectangles show the pairs of phase and amplitude frequencies used to derive average low β-broad band γ (left box) and high β-broad band γ (right box) for each subject. On the right hand side, average preferred phase of coupling for low β-broad band γ (red) and high β-broad band γ (blue). (D) Comparing average PAC between S1 and M1/PM signals indicates statistically significant difference in high β-broadband γ PAC. Asterisk (*) indicates statistical significance at $P<0.05$ (Wilcoxon signed rank test, Bonferroni correction). Each bar shows the mean (across the cohort) and 95% confidence interval of the mean.

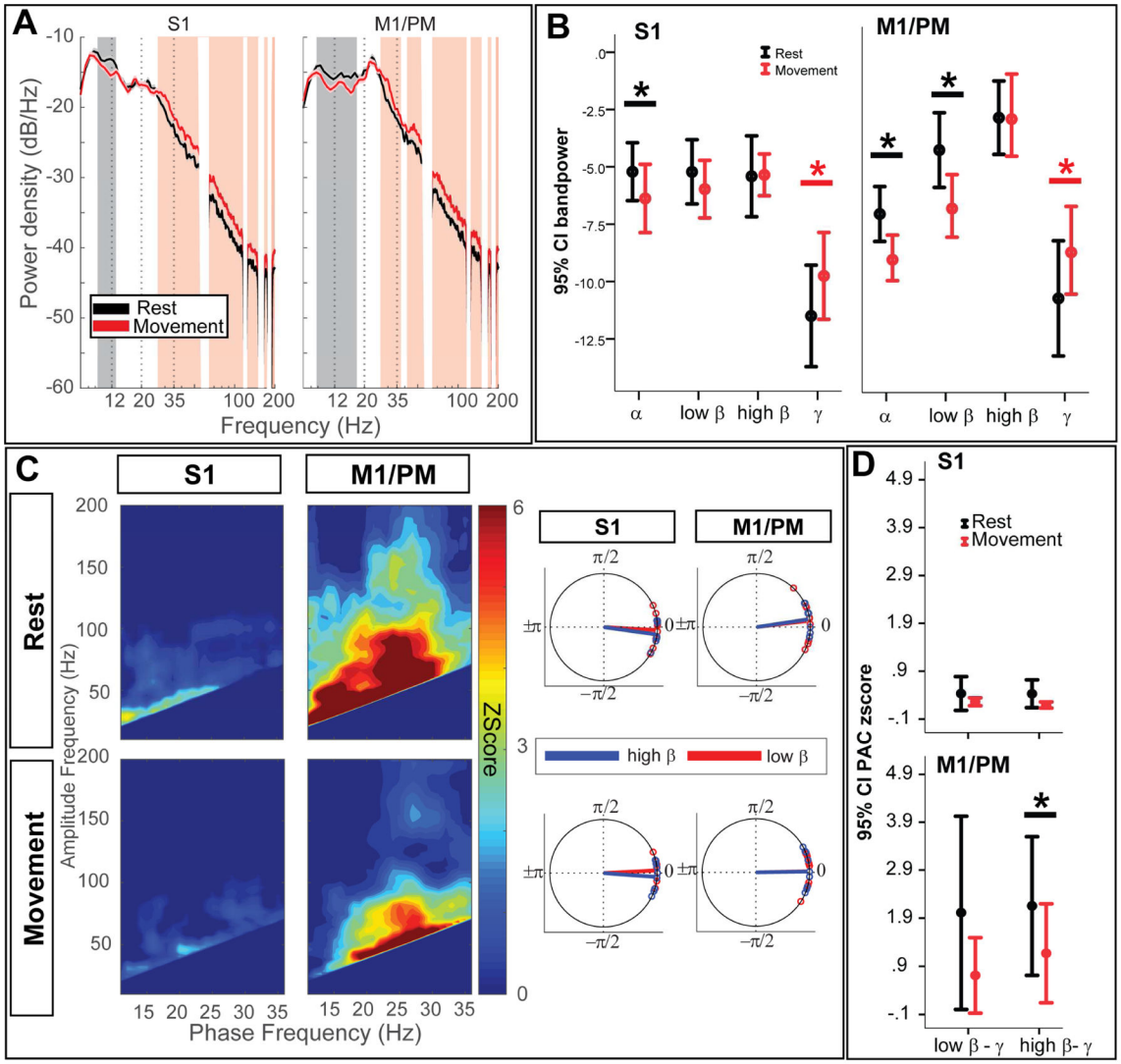

Figure 3.

Movement changes cortical power in low β and cortical PAC in high β frequencies (A) Group average PSDs are plotted for S1 (left) and M1/PM (right), in the DBS-OFF condition, during rest (black trace) and contralateral hand movement (red trace). Vertical shade represents statistically significant difference observed by two-group test of spectrum. Frequency axis is plotted in log format to magnify changes in β band. (B) Average band power values are also compared between rest (black) and contralateral hand movement (red). Asterisk (*) sign indicates statistically significant difference ($P<0.05$, tested by non-parametric Wilcoxon signed-rank test, corrected for multiple comparisons using Bonferroni). Each bar shows the mean (across the cohort) and 95% confidence interval of the mean. (C) On the left hand side, average z-score maps for the cohort are represented, during DBS-OFF recordings for rest (top row) and contralateral hand movement (bottom row). On the right hand side, average preferred phase of coupling for low β-broadband γ (red) and high β-broad band γ (blue) are represented. (D) Comparing average PAC between rest and movement indicates statistically significant suppression of high β-broadband γ PAC

at M1/PM. Asterisk (*) indicates statistical significance at $P<0.05$ (Wilcoxon signed rank test, Bonferroni correction). Each bar shows the mean (across the cohort) and 95% confidence interval of the mean.

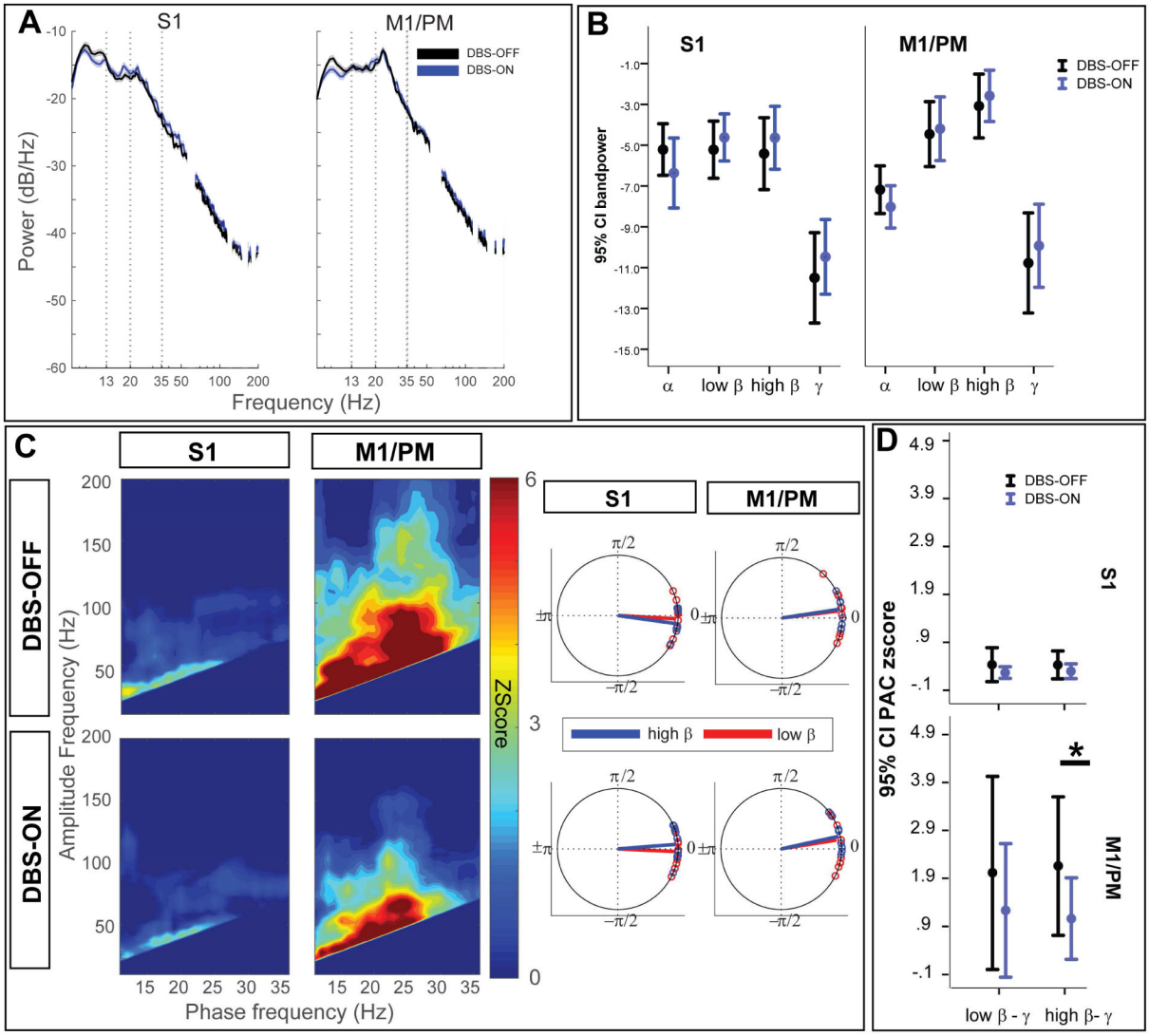

Figure 4.

During rest, GPi-DBS only modulates motor cortical PAC in high β frequencies without causing a significant power change (A) Group average PSDs are plotted for S1 (left) and M1/PM (right), in the DBS-OFF condition, during rest at DBS-OFF (black trace) and DBS-ON (blue trace). Gray shade represents statistically significant difference observed by two-group test of spectrum. No significant difference was found after correction for multiple comparisons. (B) Average band power values during resting conditon (DBS-OFF (black), DBS-ON (blue)) are also compared. Asterisk (*) sign indicates statistically significant difference ($P<0.05$, tested by non-parametric Wilcoxon signed-rank test, corrected for multiple comparisons using Bonferroni). Each bar shows the mean (across the cohort) and 95% confidence interval of the mean. (C) On the left hand side, average z-score maps for the cohort are represented, during resting condition for DBS-OFF (top row) and DBS-ON (bottom row). On the right hand side, average preferred phase of coupling for low β-broadband γ (red) and high β-broad band γ (blue) are represented. (D) Comparing average PAC between DBS-OFF and DBS-ON indicates statistically significant suppression of high

β-broadband γ PAC at M1/PM. Asterisk (*) indicates statistical significance at $P<0.05$ (Wilcoxon signed rank test, Bonferroni correction). Each bar shows the mean (across the cohort) and 95% confidence interval of the mean.

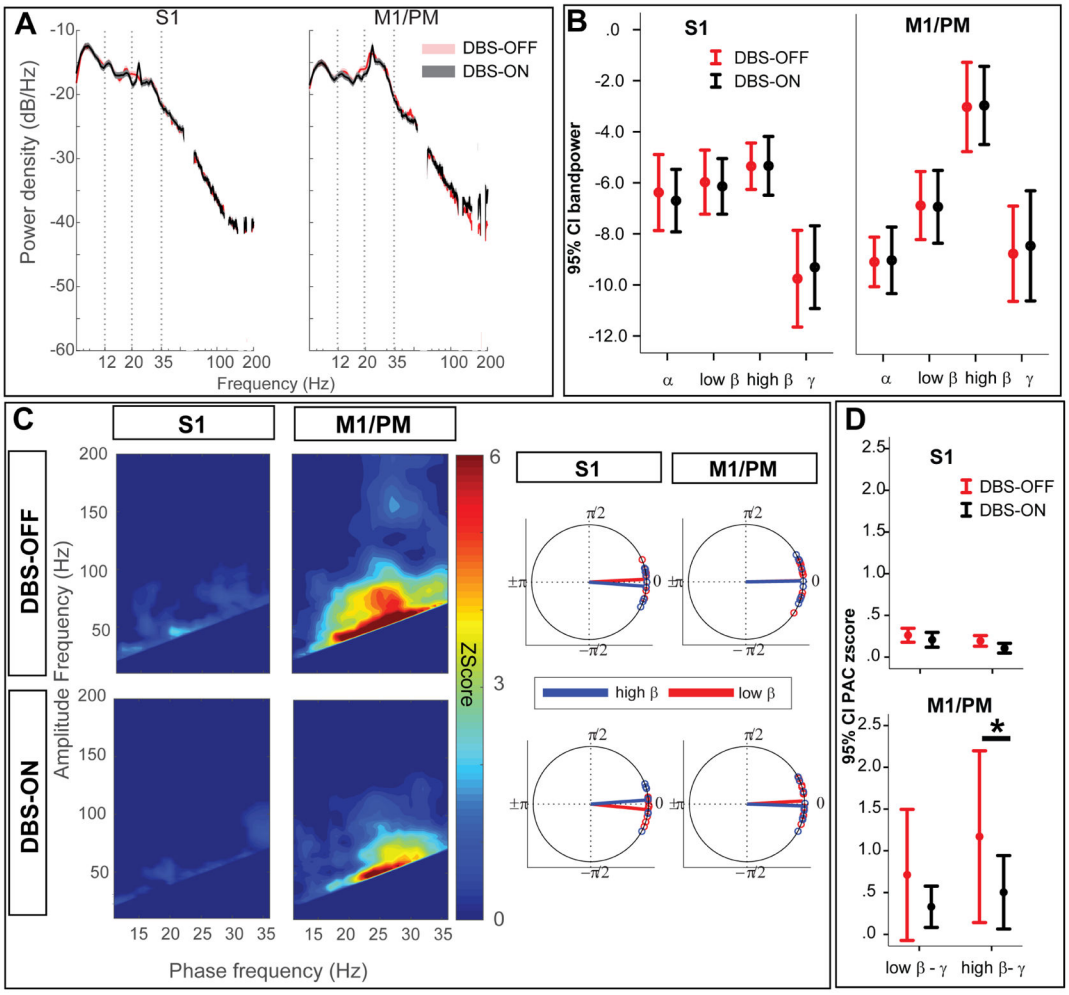

Figure 5.

During movement, GPi-DBS only modulates motor cortical PAC in high β frequencies without causing a significant power change (A) Group average PSDs are plotted for S1 (left) and M1/PM (right), in the DBS-OFF condition, during movement at DBS-OFF (red trace) and DBS-ON (green trace). Gray shade represents statistical significant difference observed by two-group test of spectrum. No significant difference was found after correction for multiple comparisons. (B) Average band power values during contralateral hand movement (DBS-OFF (red), DBS-ON (green)) are also compared. Asterisk (*) indicates statistically significant difference ($P<0.05$, tested by non-parametric Wilcoxon signed-rank test, corrected for multiple comparisons using Bonferroni). Each bar shows the mean (across the cohort) and 95% confidence interval of the mean. (C) On the left hand side, average z-score maps for the cohort are represented, during contralateral hand movement for DBS-OFF (top row) and DBS-ON (bottom row). On the right hand side, average preferred phase of coupling for low β-broadband γ (red) and high β-broad band γ (blue) are represented. (D) Comparing average PAC between DBS-OFF and DBS-ON indicates statistically significant suppression of high β-broadband γ PAC at M1/PM. Asterisk (*) indicates statistical

significance at $P<0.05$ (Wilcoxon signed rank test, Bonferroni correction). Each bar shows the mean (across the cohort) and 95% confidence interval of the mean.

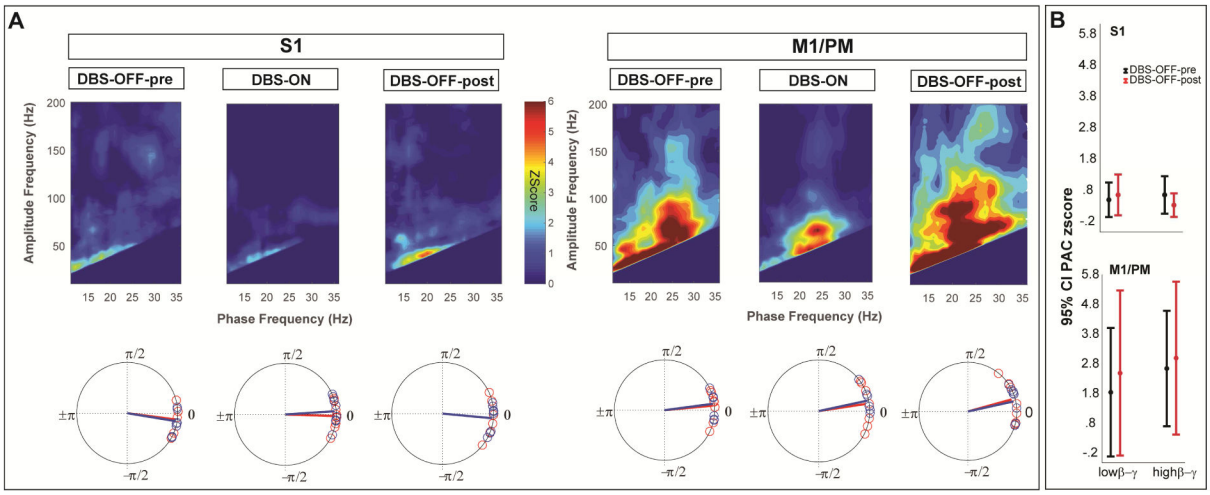

Figure 6.

Resting state cortical PAC is restored after termination of high frequency GPi-DBS (A) Average zscore maps for subgroup (N=8) of subjects with resting state recordings during DBS-OFF before high frequency stimulation (DBS-OFF-pre), high frequency stimulation (DBS-ON) and DBS-OFF after the high frequency stimulation (DBS-OFF-post), indicating the reversal of untreated state PAC in the sensorimotor cortex. Bottom row shows the average preferred phase of coupling for low β-broadband γ (red) and high β-broad band γ (blue). (B) Comparing average PAC between DBS-OFF-pre and DBS-OFF-post conditions indicated no statistically significant difference in the coupling strength between the conditions (P>0.1, Wilcoxon signed-rank test).

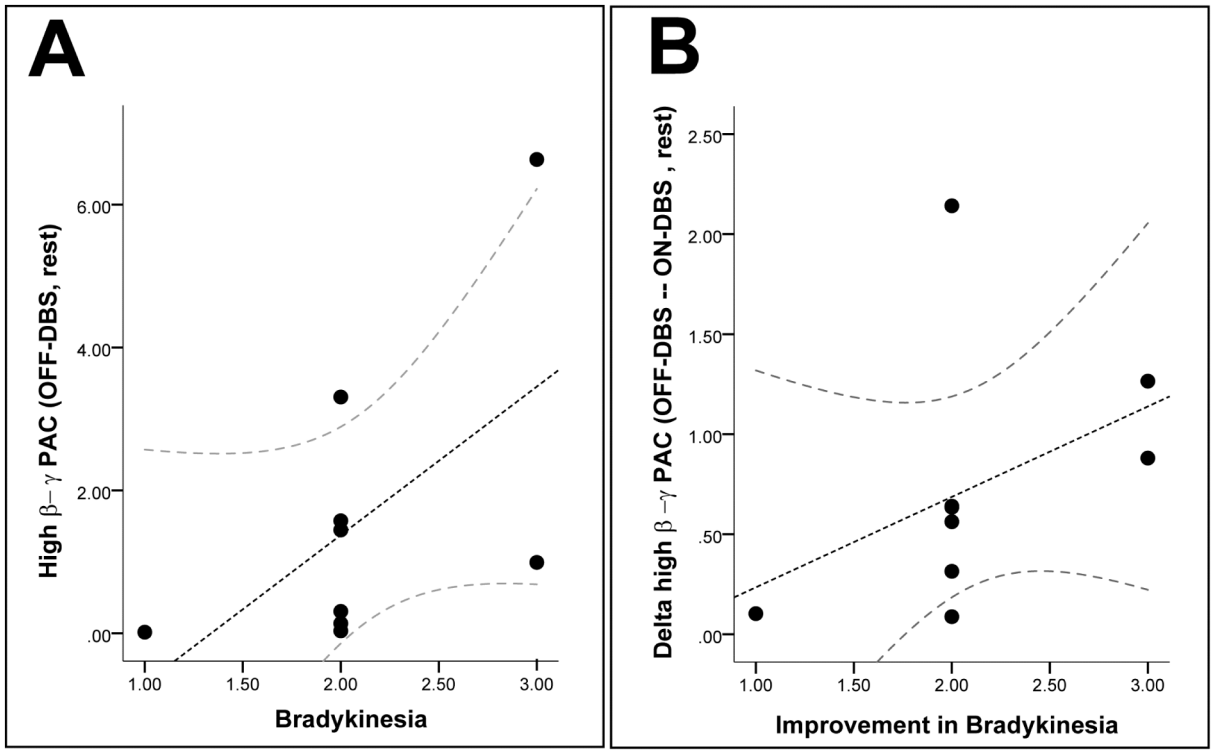

Figure 7.

Motor cortical high β-broadband γ PAC is related to disease severity (ie bradykinesia) and changes in proportion to improvement in disease symptoms once GPi-DBS is applied. (A) Scatter plots showing significant correlation between high β-broadband γ PAC at rest and in the DBS-OFF (i.e. untreated state) and bradykinesia scores. (B) Scatter plots showing significant correlation between changes in high β-broadband γ PAC at rest with GPi-DBS (i.e. treatment related changes) and improvement in bradykinesia scores.

Table 1

Demographic and clinical information

Patient	Age Gender	UPDRS III (OFF-DBS/ON-DBS)			ON-DBS stimulation parameters		
		Tremor	Rigidity	Bradykinesia	Voltage (V)	Frequency(Hz)	PulseWidth (μs)
P1	61/M	2/1	3/0	2/0	3.4	185	90
P2	72/M	0/0	3/0	3/0	3.4	185	90
P3**	76/F	NA/0	NA/0	NA/0	3.5	185	90
P4	59/M	1/0	2/0	2/0	1.8	185	90
P5	61/M	2/1	2/1	1/0	3.4	185	90
P6	73/F	0/0	3/0	3/0	2.5	185	90
P7	57/F	0/0	2/0	2/0	3	185	90
P8	55/M	0/0	3/0	2/0	3	185	90
P9*	64/F	0/0	2/0	2/0	3.4	185	90
P10	61/M	1/0	2/0	2/0	3	185	90

*This patient has mild dyskinesias that were still present during DBS-ON recordings.

**Pre-operative UPDRS measurements (off medications) were not available for this subject (P3)